

Structure, optical and magnetic behavior of nanocrystalline CuO nanopowders synthesized via a new technique using Schiff base complex

Ahmed Mourtada Elseman¹ · D. A. Rayan¹ · M. M. Rashad¹

Received: 14 September 2015 / Accepted: 12 November 2015 / Published online: 24 November 2015
© Springer Science+Business Media New York 2015

Abstract New Cu(II) Schiff base complex [Cu(L)(H₂O)Cl] have been synthesized using the sonochemical route. Then, nanocrystalline monoclinic copper oxide CuO phase were obtained from the complex by annealing the formed Cu(II) Schiff base complex at 600 °C for 2 h. The crystallite size of the formed CuO was 51.5 nm. The formed CuO sample was appeared as cubic-like structure. Besides, the band gap energy of the CuO nanoparticles was 1.39 eV. Meanwhile, the photoluminescence emission spectra measurement (PL) at different excitation bands were evinced that CuO exhibited luminescence band around at 403 nm. Indeed, the saturation magnetization (*M_s*) was 0.17 μg whereas the coercivity (*H_c*) was 233.5 Oe, indicating the weak ferromagnetic behavior of the formed CuO powders was observed. Consequently, in this paper we illustrates that the organic–inorganic compounds may be suitable precursors for synthesis of nano-scale materials. The sonochemistry method may have some advantages such as: it takes place with shorter reaction times and produces better yield.

1 Introduction

Schiff bases are considered as a very important class of organic compounds which have wide applications in many aspects as carriers in the preparation of potentiometric sensors for determining cations and anions accordingly, some Schiff bases possess chemical intermediate and

perfume bases in dyes, a catalyst in chemical reactions, rubber accelerator and in liquid crystals for electronic devices [1, 2]. Particularly, the transition metal complexes with Schiff bases as ligand are of paramount scientific interest, due to their multiple implications [3]. Otherwise, macroscopic properties of materials strongly depend on both the size and the morphologies of the microscopic particles they are made up from. This is especially true for materials with morphological features smaller than a micron in at least one dimension, which is commonly called nano-scale materials, or simply nanomaterial. In these materials the ratio of surface area to volume is vastly increased when compared to compounds with larger grain sizes and quantum mechanical effects such as the “quantum size effect” begin to play a significant role. These effects only play a minor role when going from macro to micro dimensions, but become increasingly important when reaching the nanometer size range [4]. Thus synthesis and characterization of nano-structures with different particle sizes and morphologies are very important both from the viewpoint of basic science as well as for technological applications. Nanoparticles have attracted great interest in recent years because of their unique chemical and physical properties, which are different from those of either the bulk materials or single atoms and have potential applications in optoelectronics, catalysis, and ceramics and so on [5, 6]. Among them, copper (II) oxide CuO nanopowders as an important p-type semiconductor with a narrow band gap (1.2 eV), has received great attention owing to its important properties and widespread applications [7]. Furthermore, it has been widely investigated for many optoelectronic devices such as optical switch, energy storage, field emission devices and solar cells, gas sensors, lithium-ion electrode materials, magnetic storage media, rectifiers, heterogeneous catalysts, etc. [8–10]. From the

✉ D. A. Rayan
diaa001@yahoo.com

¹ Central Metallurgical Research and Development Institute (CMRDI), P.O. Box 87, Helwan, Cairo, Egypt

best of our knowledge, the synthesis of CuO nanopowders from Schiff base complex is not mentioned elsewhere. Herein, we describe the synthesis and characterization of new copper (II) complexes of a Schiff base ligand namely 2-((pyridin-3-ylmethylene)amino)phenol. Sonochemistry is the research area in which molecules undergo a reaction due to the application of powerful ultrasonic radiation (24 kHz–10 MHz) [11]. Then, CuO nanopowders were obtained by annealing such complex at 600 °C for 2 h. The change in structure, optical and magnetic properties of the formed powders was systematically investigated.

2 Experimental

2.1 Materials

All reagents and olefins were purchased from Merck or Fluka and used as received. Solvents used for reactions were purified and dried by conventional methods [12]. 2-((pyridin-3-ylmethylene) amino) phenol was prepared according to the reported method [13, 14].

2.2 Synthesis of the 2-((pyridin-3-ylmethylene)amino)phenol (HL)

(HL) was prepared by the condensation of 3-pyridinecarboxaldehyde (1 mL, 0.01 mol) with 2-aminophenol (1.0913 g, 0.01 mol) in ethylacetate (20 mL) at 80 °C temperature under reflux for 1 h (Fig. 1a). The precipitated HL was filtered, recrystallized from methanol and dried in vacuum desiccators. The purity of products was checked by TLC on silica gel. CHN indicates that: C, 72.22 H, 4.90 N, 14.15 %. Calcd: C, 72.71 % H, 5.08 % N, 14.13 % m.p: 93 °C. FT-IR (KBr disk): 3059, 2865, 1576, 1482, 1364, 1255, 1168, 858, 754 cm^{-1} . $^1\text{H-NMR}$ in DMSO, δ ppm (mult., integ., assgmt.): 9.04 (s, ^1H , $-\text{CH}=\text{N}-$), 6.88 (d, 1H, Ar-Ha), 7.12 (t, 1H, Ar-Hb), 6.8 (t, 1H, Ar-Hc), 7.27 (d, 1H, Ar-Hd), 8.41 (d, 1H, Ar-He), 7.54 (m, 1H, Ar-Hf), 8.56 (d, 1H, Ar-Hg), 8.76 (s, 1H, Ar-Hh).

2.3 Synthesis of nano-structures HL–copper complex by sonochemical method (HL-Cu)

10 μL of a 0.1 M solution of CuCl_2 in MeOH was positioned in a high-density ultrasonic probe, operating at 40 kHz with a maximum power output of 400 W. Into this solution, 10 mL of a 0.2 M solution of the ligand HL was added dropwise. The obtained precipitate was filtered off, washed with methanol and then dried in air. CHN Found: C, 45.12 H, 3.67 N, 8.43 Cu, 20.78. Calcd: C, 45.87 H, 3.53 N, 8.92 Ni, 20.22. FT-IR (KBr disk): 3391, 3010, 2860, 1621, 1430, 1249, 1111, (685, 625) bridging, 545,

382 cm^{-1} . Figure 1 indicates the method used for preparation of CuO powders from nanometal complex.

2.4 Physical characterization

The purity of products was checked by Thin Layer Chromatography (TLC) on silica gel. The melting points of the ligand and their complexes were measured by the electrothermal melting point. An ultrasonic generator equipped with an H22 sonotrode with diameter 22 mm, operating at 24 kHz with a maximum power output of 400 W, was used for the ultrasonic irradiation. The as-prepared products were characterized using FT-IR spectroscopy using compressed with KBr as disks on a The JASCO FT/IR-6300 type A spectrometer. Proton NMR spectra were recorded in DMSO- d_6 on a Varian FT-200 MHz spectrometer using TMS. TGA were obtained on a NETZSCH STA 409 C/CD at a heating rate of 10 °C min^{-1} under air atmosphere. DSC thermograms were performed on a Mettler Toledo DSC 822e module. XRD patterns of the resulting products were identified by a Bruker D8-advance X-ray powder diffractometer with Cu $K\alpha$ radiation ($\lambda = 1.5406 \text{ \AA}$). The crystallite sizes of the produced CuO powders for the most intense peak (111) phase determined from the X-ray diffraction data using the Debye–Scherrer formula:

$$d_{RX} = k\lambda/\beta\cos\theta \quad (1)$$

where d_{RX} is the crystallite size, $k = 0.9$ is a correction factor to account for particle shapes, β is the full width at half maximum (FWHM) of the most intense diffraction peak (111) plane, λ is the wavelength of Cu target = 1.5406 \AA , and θ is the Bragg angle. The micrographs of produced samples were examined by direct observation via scanning electron microscope (SEM) model (JSM-5400, JEOL instrument, Japan). Transmission electron microscopy (TEM) of the particles was fulfilled using a JEOL-JEM-1230 microscope. The UV–Vis absorption and diffuse reflectance spectrum were recorded at room temperature using UV–Vis-NIR spectrophotometer (Jasco-V-570 spectrophotometer, Japan) fitted with integrating sphere reflectance unit (ISN) in the wavelength range 200–2000 nm. Photoluminescence (PL) spectra were recorded at room temperature with a fluorescence spectrophotometer equipped with 50 W xenon lamp (Shimadzu RF-5301PC, Kyoto, Japan). Finally, the magnetic properties of the formed powders were measured at room temperature using a VSM (7410-LakeShore, USA) in a maximum applied field of 20 kOe. From the obtained hysteresis loops, the saturation magnetization M_s , remanence magnetization M_r and coercivity H_c were determined.

3 Results and discussion

The analytical data for the complex was in good agreement with the calculated values. The complex was characterized by elemental analyses (CHN), UV–Vis and FT-IR spectroscopy. This complex was found to be soluble in methanol,

acetonitrile, dimethylformamide (DMF) and dimethyl sulfoxide (DMSO). The solid compound was stable at room temperature in air. Colour, melting point, molecular formula and elemental analysis was summarized in Table 1.

The mass spectrum of the HL and Cu-complex as depicted in Fig. 2 indicated that the molecular ion peaks at

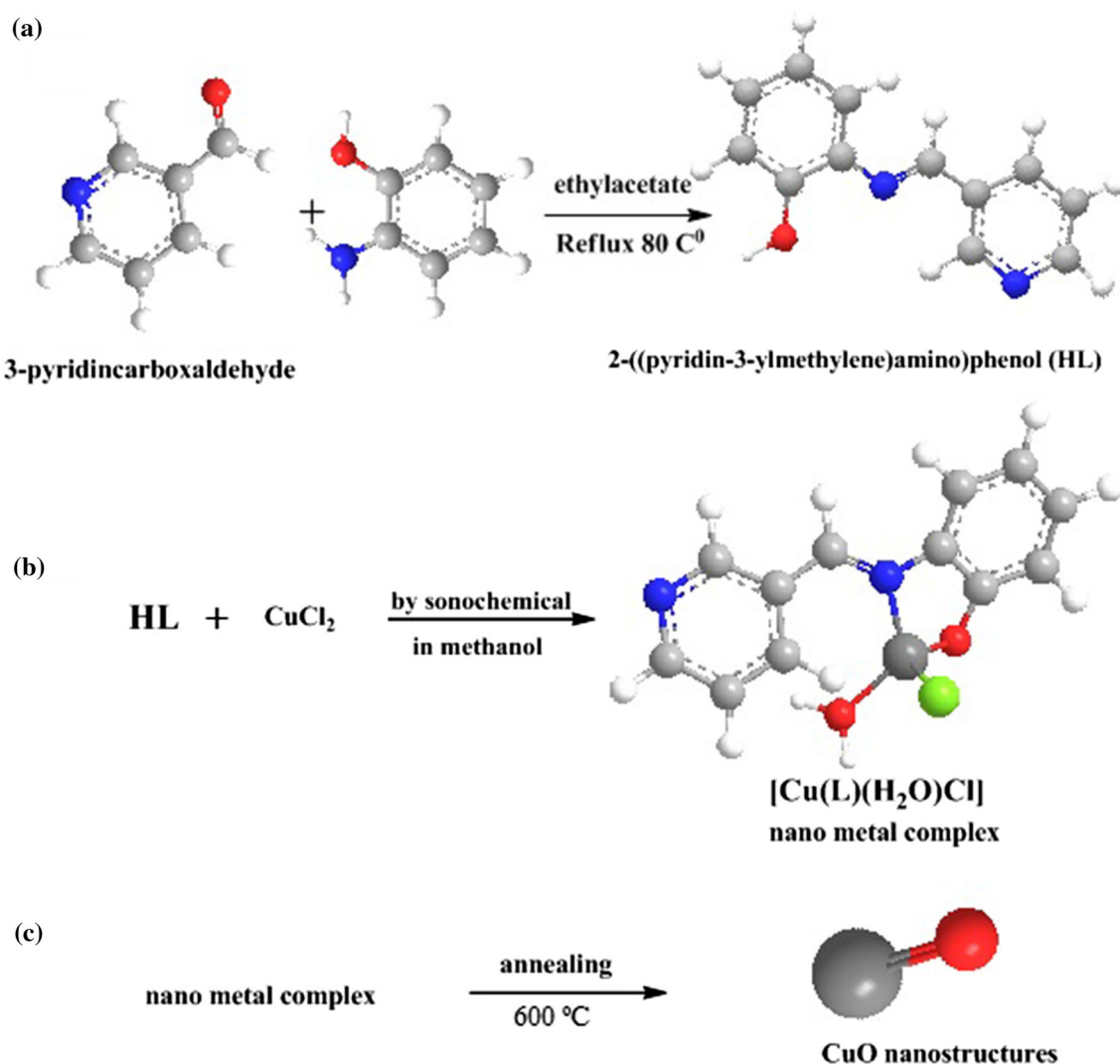


Fig. 1 a Synthesis and structure of the HL, b the formation of nano metal complex, c synthesis of CuO nanopowders

Table 1 Analytical and physical data of the HL and HL-Cu

Compound	Color	M.P	Chemical formula	Yield (%)	Elemental analysis			
					Calculated (found) (%)			
					C	H	N	M
HL	Yellow	90–93	C ₁₂ H ₁₀ N ₂ O 198.2	80	72.71 (72.22)	5.08 (4.90)	14.13 (14.55)	–
HL-Cu	Reddish brown	180–181	C ₁₂ H ₁₁ ClCuN ₂ O ₂ 314.2	76	45.87 (45.12)	3.53 (3.67)	8.92 (8.43)	20.22 (20.78)

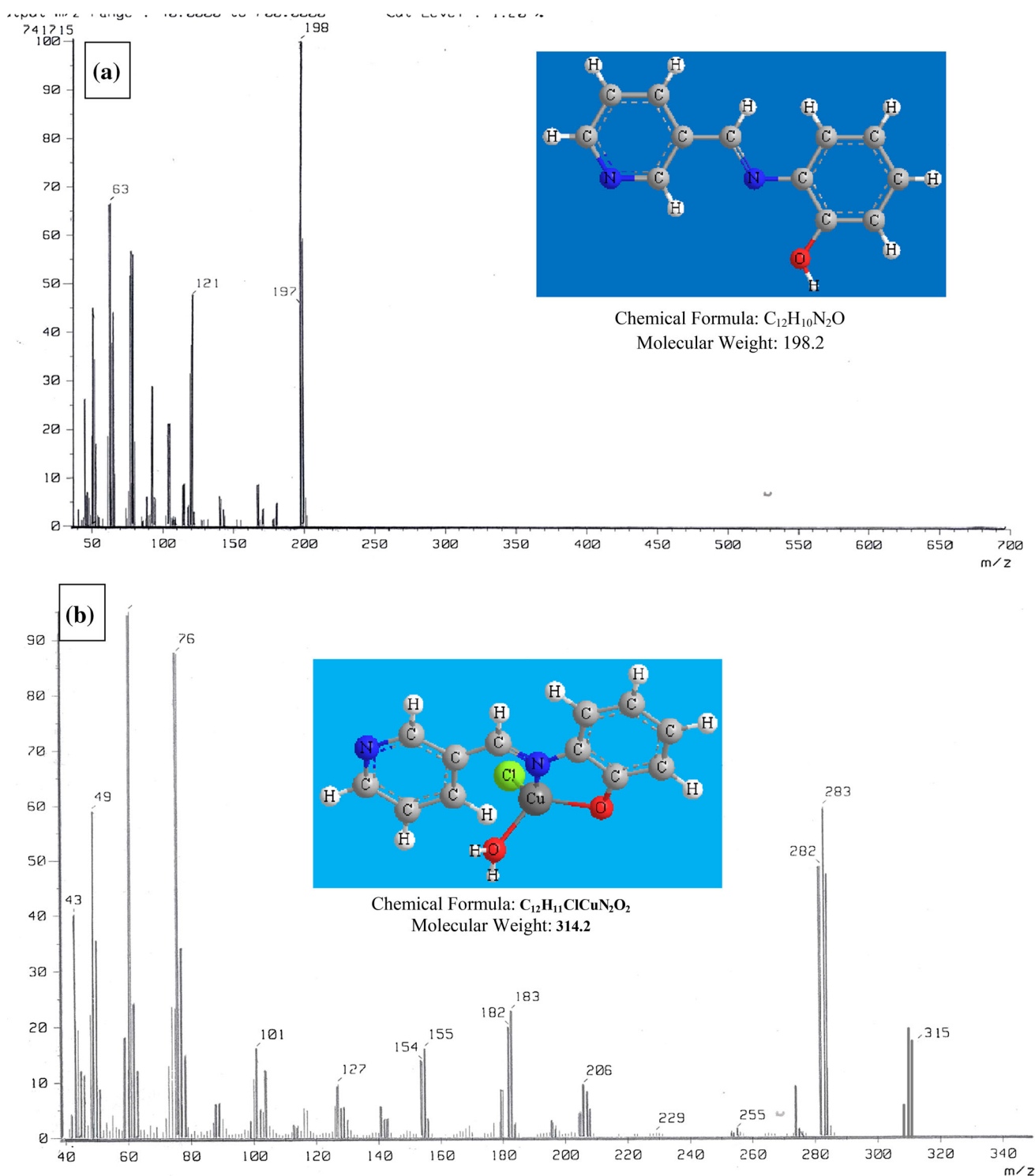


Fig. 2 The mass spectrum of **a** HL and **b** HL-Cu

Table 2 FT-IR data for prepared compounds

Compounds	Wave numbers (cm^{-1})									
	ν_{H_2O}	ν_{OH}	$\nu_{CH-arom.}$	$\nu_{CH-aliph.}$	$\nu_{C=N}$	$\nu_{C=C}$	ν_{C-O}	ν_{C-N}	ν_{M-N}	ν_{M-O}
HL	–	3318	3059	2865	1621	1482	1255	1168	–	–
Nano HL-Cu	3319	–	3011	2856	1598	1478	1295	1185	561	487

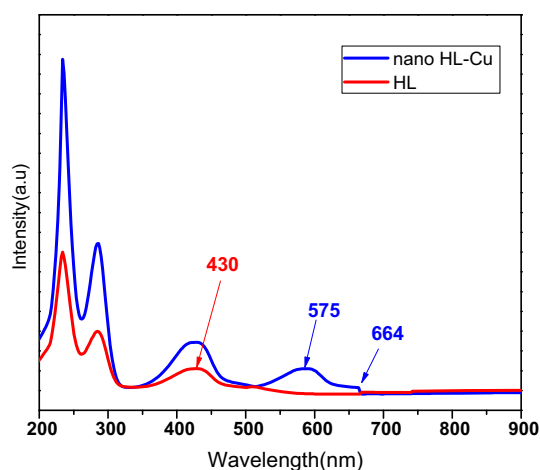


Fig. 3 UV-Vis spectra of **a** HL, and **b** nano HL-Cu

$m/z = 198.2$ and 314.2 were coincided with the molecular formula $C_{14}H_{13}NO_2$ and $C_{12}H_{11}ClCuN_2O_2$, respectively.

The FT-IR spectrums of (HL) as well as the nano HL-Cu are listed in Table 2. A very strong intense absorption band at 1621 cm^{-1} was assigned to C=N whereas the C=C band was observed at 1482 cm^{-1} through FT-IR spectra of HL [13, 14]. The presence of band of ν_{OH} at 3318 cm^{-1} was confirmed the formation of the proposed Schiff base framework. Moreover, the peak band at 1255 cm^{-1} was corresponded to ν_{C-O} . Furthermore, the similar band peak was also observed for HL-Cu complex indicating to the same structure. Besides, M–O and M–N vibrations of Cu complex were detected at 561 and 487 cm^{-1} , respectively [15]. Meanwhile, the FT-IR spectra of the Cu-complex evinced that the stretching frequency of the C=N bond was shifted to lower wave number by (23 cm^{-1}) in complexation with the free ligand after coordination. This shift was due to the reduction of the double bond character of the C=N bond, which was caused by the coordination of nitrogen to metal center. Additionally, lattice absorbed water at $3390\text{--}3200\text{ cm}^{-1}$ [16, 17].

Figure 3 illustrates the electronic absorption spectra of the complexes in DMSO at room temperature. The electronic spectra of HL and nano HL-Cu which were dissolved in DMSO have a great similarity the spectra characterized by two bands in the region 220 nm (45454.55 cm^{-1}) which it was attributed to $L_a \rightarrow A$ transitions of phenyl ring. Meanwhile, the second band which appeared at 270 nm (37037.0 cm^{-1}) was corresponded to the azomethine group $\pi\text{--}\pi^*$ and the final band observed at 430 nm (23255.81 cm^{-1}) was due to $n\text{--}\pi^*$ transition [13, 14].

On the other hand, HL-Cu complex exhibits two bands at 664 and 575 nm (15062 and 17391.3 cm^{-1}) regions. The band at 475 nm (21034 cm^{-1}) was relatively

Table 3 Electronic spectra in (DMF) and magnetic moment (B.M) of (L) and its metal complexe

Compound	λ_{max} (cm^{-1})	Assignment	μ_{eff} B.M	Suggested structure
HL	37037.0	$\pi\text{--}\pi^*$	–	–
	22222.22	$n\text{--}\pi^*$		
Nano HL-Cu	15062	${}^2T_{2g} \rightarrow {}^2E_g$	D	Square planar

D diamagnetic

to a symmetry-forbidden $L \rightarrow M$ charge transfer band [18] whereas band at 664 nm (15062 cm^{-1}) was assigned to the d–d transition corresponding to ${}^2T_{2g} \rightarrow {}^2E_g$. The band position was in agreement with those generally observed for planar copper(II) complexes [18]. Magnetic susceptibility measurement indicated that HL-Cu complex was diamagnetic in nature ($\mu_{\text{eff}} = D$) thus confirming the square planar geometry as shown in Table 3.

Figure 4 describes the ${}^1\text{H}$ NMR spectrum of HL and HL-Cu complex. HL showed signals at range $8.5\text{--}9.5\text{ ppm}$ were due to the resonance of --OH , and --N=CH-- groups as shown in Fig. 4a, the signal of OH group lying at higher field side can be attributed to the contribution of the OH group intramolecular and intermolecular hydrogen bonds. Moreover, addition of D_2O to the previous solution led to diminishing the signal due to proton exchange [19]. The resonance of imine proton downfield was shifted to 8.8 ppm due to the strong shielding effect of the hydroxyl group. Furthermore, the multiple signals lying in the range of $6.8\text{--}8.4\text{ ppm}$ were due to resonance of aromatic protons. From Fig. 4b, the observing signal of OH protons of the HL ca 9.1 ppm was not observed in any of the prepared HL-Cu complexes, which confirmed the bonding of the phenolic oxygen to the metal ions (C–O–M) [20], the other signals of the phenyl group in the free ligand and the complexes were found in the expected regions. The broad signal at ca 3.4 ppm in the copper (II) complexes was also assigned to the water of crystallization.

Figure 5 shows SEM image of the formed Cu complex. It can be observed that the formed was exhibited cubic like structure. Additionally, the EDX spectrum illustrates that the Cu complex was composed from Cu, O, N and Cl which confirmed the formation of the complex [21].

Thermal decomposition of the nano-sized structures of HL-Cu in air at $600\text{ }^\circ\text{C}$ for 2 h produced monoclinic CuO nano-structures. Figure 6 illuminates XRD diffraction profile of CuO powders. It is clear the peaks match well with those of the monoclinic CuO (JCPDF No. 73-1917). XRD pattern showed sharp peaks which indicated the well crystallinity of CuO synthesized. No characteristic peaks of impurities are detected in the XRD pattern. The broadening

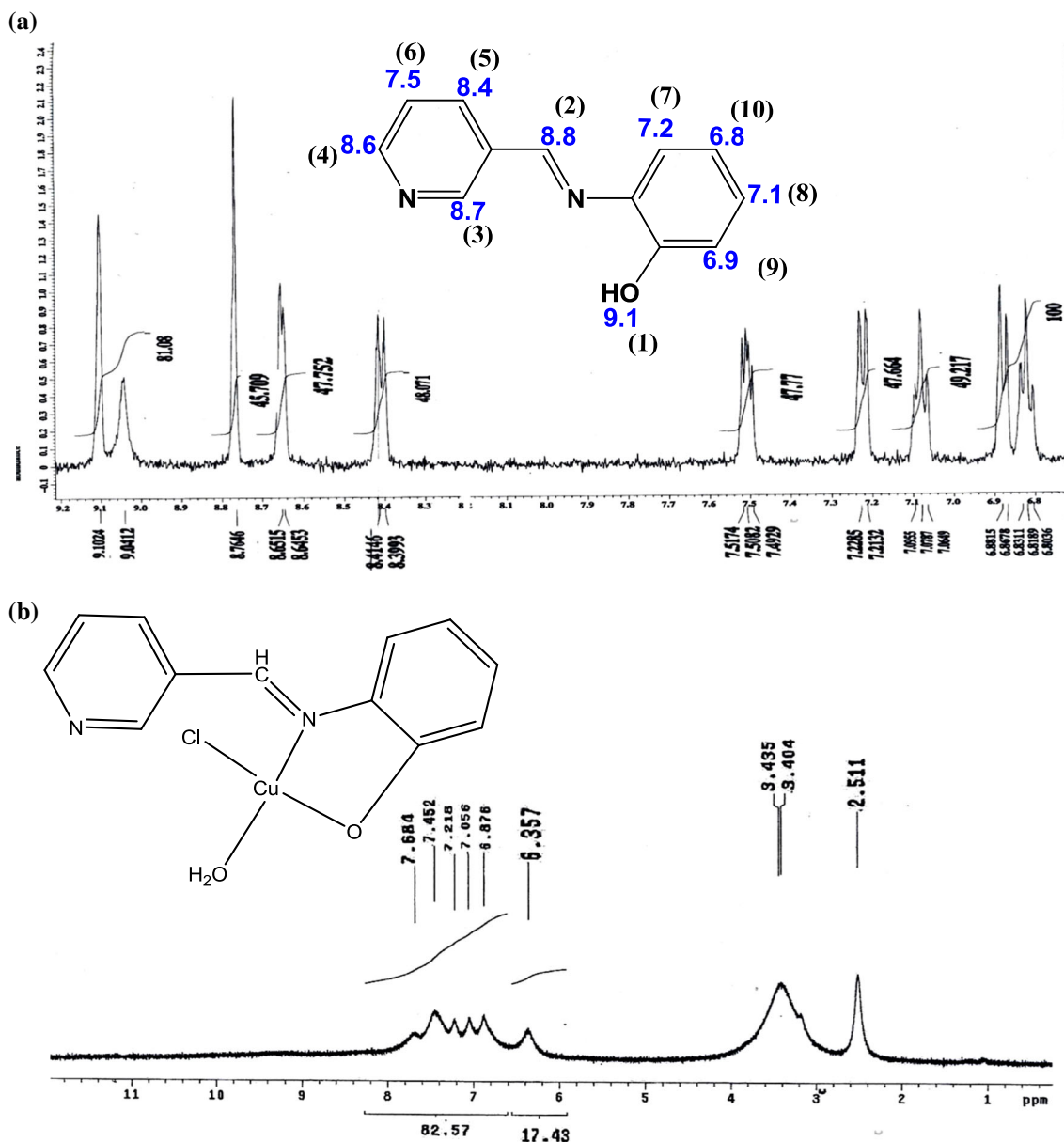


Fig. 4 a ¹H NMR spectrum of HL, b ¹H NMR spectrum of nano HL-Cu

of the peaks indicated that the particles were of nanometer scale. Moreover, XRD was matched the crystallite size of the formed powders base on Debye–Scherrer equation was 51.5 nm. The peak widths and intensities clearly indicate that copper (II) oxide was highly crystalline in nature. The lattice parameters a, b and c were calculated by applying the following equation:

$$\frac{1}{d^2} = \frac{1}{\sin^2 B} \left(\frac{h^2}{a^2} + \frac{k^2 \sin^2 B}{b^2} + \frac{l^2}{c^2} - \frac{2hl \cos B}{ac} \right) \quad (2)$$

The extracted diffraction peaks could be indexed to a monoclinic phase of CuO (S.G.: C2/c) and the lattice parameters were studied $a = 4.686 \text{ \AA}$, $b = 3.425 \text{ \AA}$, and

$c = 5.130 \text{ \AA}$, $\beta = 99.46^\circ$ and cell volume $V_{cell} = 80.946 \text{ \AA}^3$. The absence of any other by product indicated the purity of the sample. The X-ray density or theoretical density was estimated using the relation [22]:

$$\rho_x = \frac{\sum A}{N_x V} \quad (3)$$

where A is sum of the atomic weights of all the atoms in the unit cell, V is volume of the unit cell and N is the Avogadro’s number.

The surface morphology of copper oxide nanopowders were investigated using SEM and TEM micrographs as shown in Fig. 7. The SEM image of the unpassivated

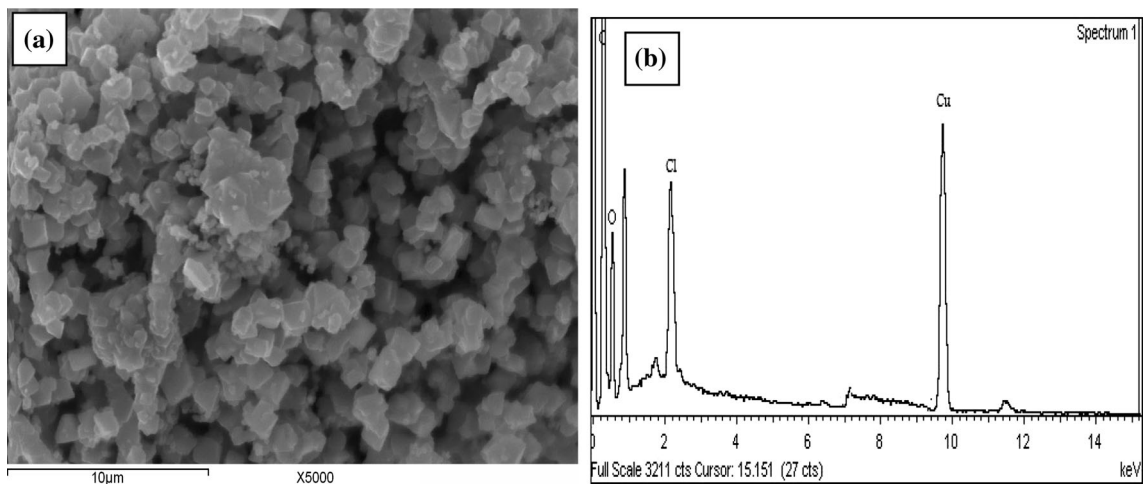


Fig. 5 **a** SEM image of Cu complex, **b** EDX spectrum analysis of Cu complex

Fig. 6 XRD patterns with structure refinement of produced CuO powders

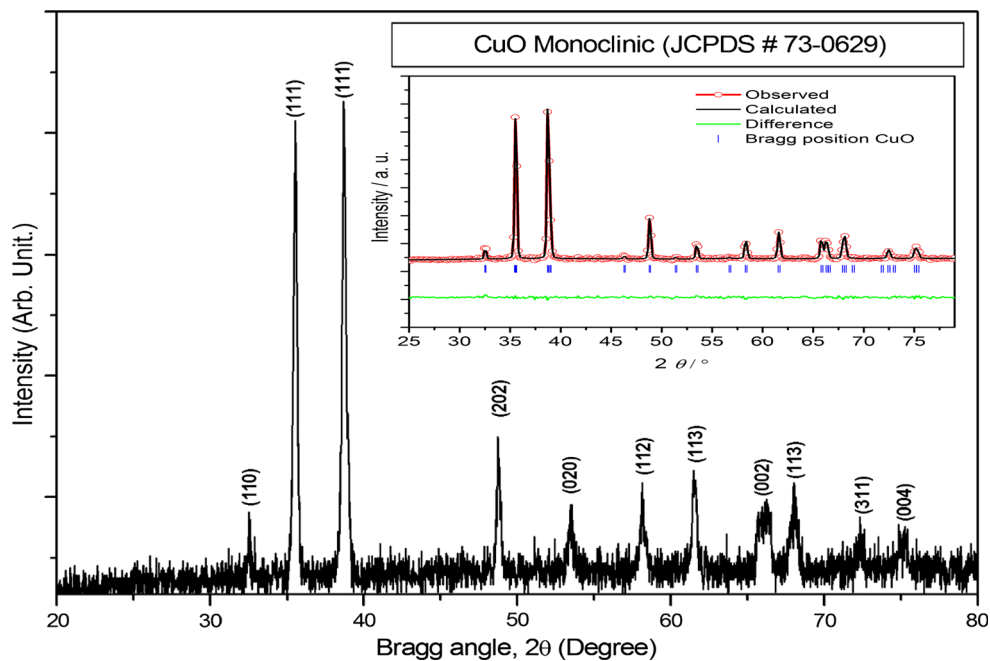
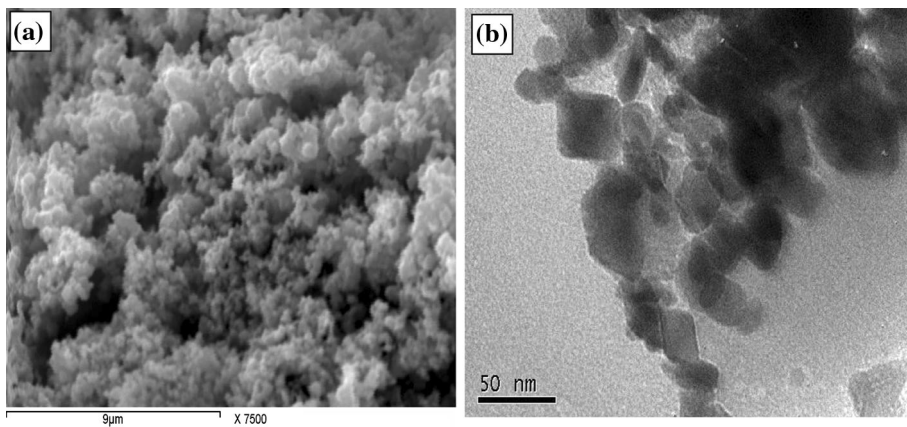


Fig. 7 **a** SEM and **b** TEM micrographs of CuO nanopowders



nanoparticles was found to be aggregated as shown in Fig. 7a. However, TEM micrograph indicated that CuO sample was the formed almost monoclinic with 30–55 nm diameter with some encapsulated.

Figure 8 represents FT-IR spectrum of the synthesized CuO nanopowders with the peak fit computer fitting in the wave number range from 800 to 400 cm^{-1} . There were no characteristic absorption bands in the region $>800 \text{ cm}^{-1}$. The DE convolution bands of FT-IR spectra that studied glass yielded the central position, amplitude, area and the full width at half maximum (FWHM) of each peak. The peaks of CuO sample was shown three broad absorption peaks at 589, 535 and 478 cm^{-1} , assigned to the stretching vibrations of Cu–O bond in the monoclinic CuO [23].

The optical properties were studied by recording the diffuse reflectance and absorption spectrum of the formed powder in the wavelength range 200–2000 nm using UV–Vis–NIR spectrophotometer using integrating sphere unit and the results are indicated in Fig. 9. Clearly, the optical

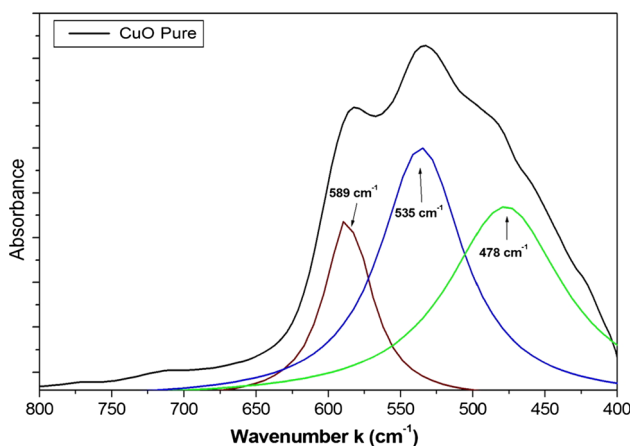


Fig. 8 FTIR absorption spectrum and deconvolution of CuO nanoparticles

reflectance of the CuO nanostructure was found to exhibit the optical absorption was the highest absorption band around 0.5–1 *a.u.*, and the lowest optical reflectivity of around 10–35 % was in visible region and near-infrared, respectively which was characteristic peak of Cu^+ and Cu^{2+} ions. The sharp rise in the absorption curve below 780 nm was confirmed the highly crystalline and mono-phase of CuO nanoparticles. These bands were assigned to octahedral symmetry copper ion due to three bands relating to ${}^2B_{2g} \rightarrow {}^2B_{1g}$, ${}^2A_{1g} \rightarrow {}^2B_{1g}$ and ${}^2E_g \rightarrow {}^2B_{1g}$ energy transitions [24, 25]. The first two transitions are very close in energy and often appear in the form of one broad band profile in the near-infrared and third band may be observed in the visible region [26, 27]. It is known that the diluted copper ions inside exhibit a broad optical absorption band around 780 nm, assigned to the ${}^2E_g \rightarrow {}^2B_{1g}$ transition due to Jahn–Teller splitting of d levels of copper ions in a ligand field [28].

The absorption co-efficient (α) values calculated from the absorption data using the relation [29, 30]:

$$\alpha(v) = (1/d) \ln(I_o/I) = (100 - R)/(2R) \tag{4}$$

where $\ln(I_o/I)$ is the absorbance (*A*), and *d* is the thickness of the sample. The reflectivity *R* can be transformed into a value proportional to the absorption using the Kubelka–Munk function [31]:

$$(hvF(R\infty))^n = A(hv - E_g) \tag{5}$$

A plot of $(\alpha hv)^2$ versus *hν* Fig. 9 was linear the absorption edge confirming the direct band gap energy in CuO nanopowders. Extrapolating the straight line portion of these plots to the *hν* axis and from the point of intersection on the *hν* axis, band gap values 1.39 eV.

Figure 10 displays photoluminescence (PL) emission and excitation spectra of CuO nanopowders at room temperature. The emission spectra measurements at different excitation bands (330, 470, 700 and 740 nm). The PL

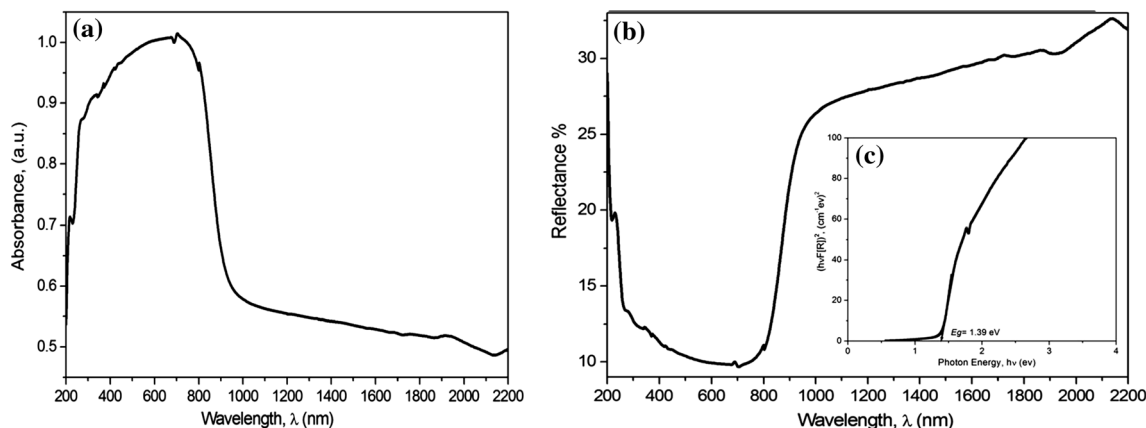


Fig. 9 Optical Properties of CuO nanopowders **a** absorbance, **b** diffuse reflectance spectra and **c** optical band gap energy

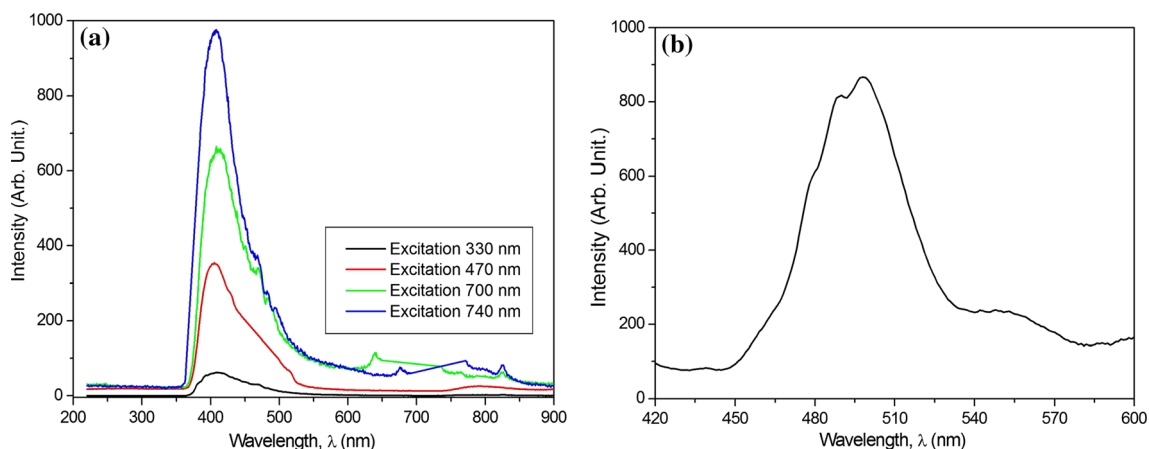


Fig. 10 Photoluminescence spectra of CuO nanopowders **a** emission spectrums with various excitation bands and **b** excitation spectrum at Emission band 400 nm

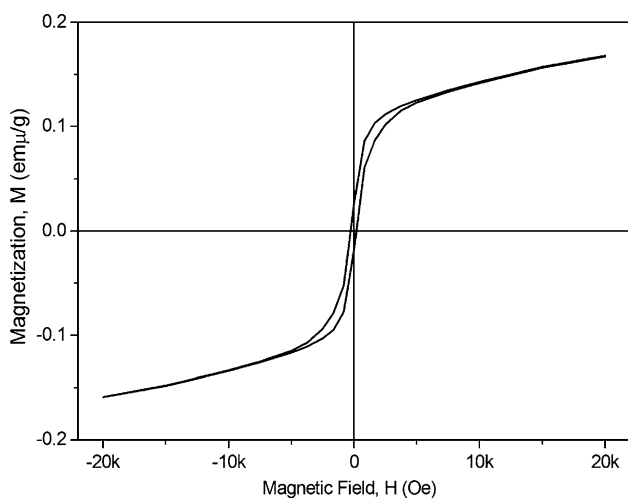


Fig. 11 Magnetic properties of CuO nanopowders

intensities of these four spectra are quite comparable to each other. The CuO was exhibited a broad violet luminescence band around 403 nm (3.08 eV) with a broad tail in the green spectral region. Obviously, CuO was also showed the similarly broad luminescence band with a broad pronounced shoulder peak in the blue–green spectral region of CuO nanopowders.

The absorbance, emission and excitation spectrums of CuO nanoparticles were indicated that the optical band gap value can be used for optoelectronic devices such as optical switch, energy storage, field emission devices and solar cells and photocatalysts.

Figure 11 shows the magnetic hysteresis curves of product CuO nanopowders measured with a VSM at room temperature at applied field 20 kOe. The value of magnetization saturation (M_s), remanence magnetization (M_r) and

coercivity (H_c) of CuO nanoparticles were 0.17, 0.02 μg and 233.5 Oe respectively, which is higher than that of 0.10 μg published before for CuO [30, 31]. This variation may be as a result of anisotropy of nanoparticles and dipolar interaction among nanoparticles.

4 Conclusion

The Schiff base ligand copper complex, where HL is 2-((pyridin-3-ylmethylene)amino)phenol, have been prepared. Nano-sized Cu complex was obtained by ultrasonic irradiation in methanol solution method. Elemental analyses (CHN), UV–Vis, FTIR spectroscopy and $^1\text{H-NMR}$ spectra evinced the formation of the Schiff base ligand copper complex. Annealing of copper complex under air at 600 $^\circ\text{C}$ for 2 h produced nano-sized monoclinic CuO structures. The monoclinic CuO particles have small size of crystalline 51.5 nm and the lattice parameters, cell volume and X-ray density or theoretical were measured. Microstructure using SEM images of the unpassivated nanoparticles was aggregated and TEM images were almost monoclinic with 30–55 nm diameter. Meanwhile, the diffuse reflectance and absorption spectra of the CuO nanostructure was shown to exhibit the optical absorption is highest absorption band in visible region and near-infrared red. The optical band gap energy of the monoclinic CuO nanoparticles using the Kubelka–Munk function was 1.39 eV. Emission spectra at different excitation bands were showed four spectra were quite comparable to each other and the sintered CuO exhibits luminescence band around at 403 nm. The saturation magnetization (M_s) was 0.16 μg whereas the coercivity (H_c) was determined to be 233.53 Oe, indicating of a paramagnetic behavior.

References

1. A.S. Gaballa, M.S. Asker, A.S. Barakat, S.M. Teleb, Synthesis, characterization and biological activity of some platinum(II) complexes with Schiff bases derived from salicylaldehyde, 2-furaldehyde and phenylenediamine. *Spectrochim. Acta A* **67**(1), 114–121 (2007)
2. A.M. Hassan, A.M. Nassar, N.M. Ibrahim, A.M. Elsamani, M.M. Rashad, An easy synthesis of nanostructured magnetite-loaded functionalized carbon spheres and cobalt ferrite. *J. Coord. Chem.* **66**(24), 4387–4398 (2013)
3. A. Pui, C. Policar, J.P. Mahy, Electronic and steric effects in cobalt Schiff bases complexes: Synthesis, characterization and catalytic activity of some cobalt(II) tetra-halogen-dimethyl salen complexes. *Inorg. Chim. Acta.* **360**, 2139–2144 (2007)
4. H.H. Nalwa, *Handbook of Nanostructured Materials and Nanotechnology*, vol. 1–5 (Academic Press, Boston, 2000)
5. A. Morsali, H.H. Monfared, A. Morsali, Syntheses and characterization of nano-scale of the Mn(II) complex with 4'-(4-pyridyl)-2,2':6',2''-terpyridine (pyterpy): the influence of the nano-structure upon catalytic properties. *Inorg. Chim. Acta* **362**(10), 3427 (2009)
6. M.M. Rashad, D.A. Rayan, K. El-Barawy, Hydrothermal synthesis of Mn doped ZnS nanoparticles. *J. Phys: Conf. Ser.* **200**, 072077 (2010)
7. Y. Mu, J. Yang, S. Han, H. Hou, Y. Fan, Syntheses and gas-sensing properties of CuO nanostructures by using [Cu(pbbt)Cl₂]₂ CH₃OH as a precursor. *Mater. Lett.* **64**(11), 1287–1290 (2010)
8. Y. Wang, T. Jiang, D. Meng, J. Yang, Y. Li, Q. Ma, J. Han, Relationship between nature of metal-oxide contacts and resistive switching properties of copper oxide thin film based devices. *Appl. Surf. Sci.* **317**, 414–421 (2014)
9. Z. Hu, H. Liub, Three-dimensional CuO microflowers as anode materials for Li-ion batteries. *Ceram. Int.* **41**, 8257–8260 (2015)
10. B. Singh, B.R. Mehta, Relationship between nature of metal-oxide contacts and resistive switching properties of copper oxide thin film based devices. *Thin Solid Films* **569**, 35–43 (2014)
11. A. Askarinezhad, A. Morsali, Syntheses and characterization of CdCO₃ and CdO nanoparticles by using a sonochemical method. *Mater. Lett.* **62**(3), 478–482 (2008)
12. D.D. Perrin, W.L.F. Armarego, *Purification of laboratory chemicals*, 3rd edn. (Pergamon, Oxford, 1980), pp. 68–174
13. M.M. Rashad, A.M. Hassan, A.M. Nassar, N.M. Ibrahim, A. Mourtada, A new nano-structured Ni(II) Schiff base complex: synthesis, characterization, optical band gaps, and biological activity. *Appl. Phys. A* **117**(2), 77–890 (2014)
14. H. Ünver, Z. Hayvali, Synthesis, spectroscopic studies and structures of square-planar nickel(II) and copper(II) complexes derived from 2-(Z)-[furan-2-ylmethyl]imino]methyl}-6-methoxyphenol. *Spectrochim. Acta A* **75**, 782–788 (2010)
15. S. Chandra, U. Kumar, Spectral studies of coordination compounds of cobalt(II) with thiosemicarbazone of heterocyclic ketone. *Spectrochim. Acta A* **62**, 940–944 (2005)
16. L.J. Bellamy, *The Infrared Spectra of Complex Molecules* (Chapman and Hall, London, 1978)
17. K. Bahgat, A.S. Orabi, Physical characteristics, vibrational spectroscopy and normal-coordinate analysis of 2-aminophenol and 2-phenylenediamine complexes. *Polyhedron* **21**(9–10), 987–996 (2002)
18. A.A.D. Paggio, D.R. McMillin, Substituent effects and the photoluminescence of Cu(PPh₃)₂(NN)⁺ systems. *Inorg. Chem.* **22**, 691–692 (1983)
19. M. El-behery, H. El-twigry, Synthesis, magnetic, spectral, and antimicrobial studies of Cu(II), Ni(II) Co(II), Fe(III), and UO₂(II) complexes of a new Schiff base hydrazone derived from 7-chloro-4-hydrazinoquinoline. *Spectrochim. Acta A* **66**, 28–36 (2007)
20. S.R. Patil, U.N. Kantank, D.N. Sen, Some ferrocenyl aroyl hydrazones and their copper(II) complexes. *Inorg. Chim. Acta* **63**, 261–265 (1982)
21. K. Raja, P.S. Ramesh, D. Geetha, Synthesis, structural and optical properties of ZnO and Ni-doped ZnO hexagonal nanorods by Co-precipitation method". *Spectrochim. Acta A* **120**, 19–24 (2014)
22. M.M. Rashad, D.A. Rayan, A.O. Turkey, M.M. Hessien, Effect of Co²⁺ and Y³⁺ ions insertion on the microstructure development and magnetic properties of Ni_{0.5}Zn_{0.5}Fe₂O₄ powders synthesized using co-precipitation method. *J. Magn. Magn. Mater.* **374**, 359–366 (2015)
23. D.A. Rayan, Y.H. Elbashar, A.B. El Basaty, M.M. Rashad, Infrared spectroscopy of cupric oxide doped barium phosphate glass. *J. Pharm. Biol. Chem. Sci. (RJPBCS)* **6**(3), 1026–1030 (2015)
24. C.J. Ballhausen, *Introduction Ligand Field Theory* (McGraw-Hill Book Co., Inc., New York, 1962)
25. D.A. Rayan, Y.H. Elbashar, M.M. Rashad, A. El-Korashy, Optical spectroscopic analysis of cupric oxide doped barium phosphate glass for bandpass absorption filter. *J. Non-Cryst. Solids* **382**, 52–56 (2013)
26. A.B.P. Lever, Series: Studies in physical and theoretical chemistry, in *Inorganic Electronic Spectroscopy*, 2nd edn, vol. 33 (1984)
27. B.J. Hathaway, D.E. Billing, The electronic properties and stereochemistry of mono-nuclear complexes of the copper(II) ion. *Coord. Chem. Rev.* **5**, 143–207 (1970)
28. P.I. Paulose, G. Jose, V. Thomas, G. Jose, N.V. Unnikrishnan, M.K.R. Warriar, Spectroscopic studies of Cu²⁺ ions in sol-gel derived silica matrix. *Bull. Mater. Sci.* **25**(1), 69–74 (2002)
29. E.M.M. Ewais, D.H.A. Besisa, A.A.M. El-Amir, S.M. El-Sheikh, D.E. Rayan, Optical properties of nanocrystalline magnesium aluminate spinel synthesized from industrial wastes. *J. Alloys Compd.* **649**, 159–166 (2015)
30. M.M. Rashad, D.A. Rayan, A.A. Ramadan, Optical and magnetic properties of CuO/CuFe₂O₄ nanocomposites. *J. Mater. Sci. Mater. Electron.* **24**, 2742–2749 (2013)
31. M.M. Rashad, S. Soltan, A.A. Ramadan, M.F. Bekheet, D.A. Rayan, Investigation of the structural, optical and magnetic properties of CuO/CuFe₂O₄ nanocomposites synthesized via simple microemulsion method. *Ceram. Int.* **41**(9), 12237–12245 (2015)